SIGNAL TRANSMISSION CHARACTERISTICS IN STRIPLINE-TYPE BEAM POSITION MONITOR

T. Suwada*, KEK, Tsukuba, Ibaraki 305-0801, Japan

Abstract

A new stripline-type beam position monitor (BPM) system is under development at the KEK electron/positron injector linac in order to measure transverse beam positions with a high precision less than 10 μm towards the Super KEKB-factory (SKEKB) [1] at KEK. The new stripline-type BPMs with a large aperture compared with previously designed BPMs have been designed for the installation in the positron capture section. In this report, the basic design for the fabrication of the prototype BPM, the theoretical analysis, and the experimental investigation on the signal transmission characteristics and its performance are in detail described on the base of a coupled-mode analysis in uniform transmission lines.

INTRODUCTION

A stripline-type BPM is a well-known beam diagnostics device to measure transverse beam positions in a plane perpendicular to the beam axis. There are many excellent review articles on this subject (see, for example, [2, 3]). In general, a stripline-type BPM has four stripline electrodes which are mounted on the inner surface of a circular pipe with $\pi/2$ rotational symmetry. The upstream port of the stripline electrode is a signal pickup and the downstream port may be short- (or 50-Ω-) terminated to the pipe ground or left open.

When a charged-particle beam passes through the BPM, a characteristic signal with bipolar shape is induced on all the stripline electrodes due to electromagnetic coupling between the electrodes and the beam. The induced signals are fed into a detection electronics through vacuum-feedthrough pickups, and the signal intensities are measured by the detection electronics. The transverse beam positions can be obtained by calculating a weighted average of the four signal intensities based on algebraic calculations. This is a basic principle on measuring transverse beam positions with a stripline-type BPM.

The signal intensity induced on each stripline electrode can be generally analyzed based on a so-called wall-current model [2], in which the wall current is a mirror current induced on the stripline electrode. Based on this model, the signal intensity may be proportional to the intensity of the wall current, that is, the beam charges, and also proportional to the angular width of the stripline electrode. Such the analysis may be fundamentally based on an electrostatic model taking into account only electrostatic coupling between the stripline electrodes and the beam.

In conventional stripline-type BPMs, there are some va-

---
* tsuyoshi.suwada@kek.jp

rieties in spatial configuration and mechanical structure of the stripline electrodes which are mounted on the inner surface of the BPM. The stripline electrode with a finite angular width viewed from the beam may be mounted with a certain gap between the electrode and the inner surface of the pipe. In such a mechanical configuration, not electrostatic coupling but electromagnetic coupling may dynamically arise between the electrodes and also between the electrodes and the beam, and thus, the signal intensities may change to some extent from the wall-current model.

From another point of view on a signal-gain calibration in a stripline-type BPM, it is important to analyze the electromagnetic coupling strengths between the stripline electrodes. An excellent calibration procedure has been implemented to stripline-type BPMs by Medvedko et al. of SLAC [4]. In this calibration procedure, an on-board calibrator embedded in the detection electronics sends its calibration signal to one of the electrodes. When the calibration signal is fed into the electrode, similar bipolar signals are induced on the other electrodes due to electromagnetic coupling. The induced signal goes back to the corresponding channel in the detection electronics in which the signal intensity is precisely measured. Thus, in such a calibration procedure, not only the signal gains in the detection electronics but also the transmission losses in entire transmission lines including the stripline electrodes themselves can be calibrated with high precision. Thus, this new calibration procedure make use of electromagnetic coupling between the stripline electrodes of the BPM.

Although electromagnetic coupling between the stripline electrodes is an important physical phenomena in the stripline-type BPM, only a few analyses have been performed to investigate the signal transmission characteristics taking into account electromagnetic coupling between the electrodes. A new analysis on the signal transmission characteristics with electromagnetic coupling between the electrodes are presented in this article. The new analysis exploits a similar method developed in microstripline circuits with electromagnetic coupling. Based on the new analysis, the signal transmission characteristics in the stripline-type BPM is systematically investigated in frequency domain along with experimental verification.

STRIPLINE-TYPE BEAM POSITION MONITOR

A new stripline-type BPM with a large aperture is shown in Fig. 1. This BPM is under development for the new positron beam line so as to reduce the beam losses in the positron transmission as small as possible. The mechanical structure of the BPM is a conventional stripline-type
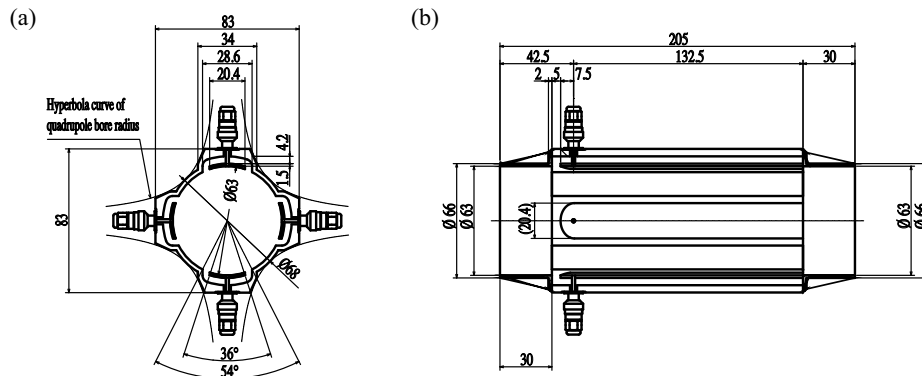
(a) (b)

Figure 1: Mechanical drawings of the prototype new stripline-type BPM, (a) in front view and (b) in side view.

BPM with $\pi/2$ rotational symmetry. The development of the present stripline-type BPM previously designed was reported elsewhere [5]. The requirements for the new BPM is that (i) firstly, the aperture diameter must be as large as possible and the diameter is required to be larger than 60 mm, and (ii) secondly, the outer diameter of the BPM must be 68 mm so that the BPM body can be precisely mounted inside a bore of a quadrupole magnet.

Based on these requirements, in order to enlarge the aperture diameter of the BPM, the four electrodes have been symmetrically mounted to the inner surface of the pipe with a same diameter, while the electrodes of the present BPM were designed to be protruded away from the inner surface of the pipe with a different diameter [5]. The electrode length is 132.5 mm and the angular width of the electrode is 36º. The characteristic impedance of the stripline electrode has been designed to be $\sim$50 Ω so as to match a characteristic impedance of the signal transmission line. The upstream end of the electrode is a signal-pickup port comprised a 50-Ω SMA-type vacuum-feedthrough while the downstream port is short-terminated to the pipe ground. The main mechanical design parameters are summarized in Table 1.

Table 1: Main Mechanical Design Parameters of the Prototype BPM

Design parameter		unit
[Electrode]		
Inner diameter	63	mm
Thickness	1.5	mm
Angular width	36	º
Gap length	4.2	mm
[Body]		
Inner diameter	63	mm
Outer diameter	68	mm

SIGNAL TRANSMISSION CHARACTERISTICS

Electromagnetic Coupling Between the Stripline Electrodes

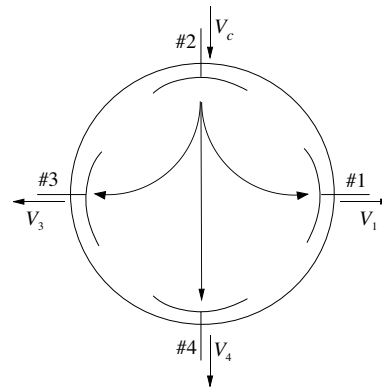A principal picture in electromagnetic coupling between the stripline electrodes is shown in Fig. 2. For example,

Figure 2: Principal picture of electromagnetic coupling between the stripline electrodes of the BPM in the front view.

when a calibration signal (V_c) is directly sent to a specific electrode (#2) from a detection electronics through a coax cable, bipolar signals are induced in the other electrodes #1 (V_1), #3 (V_3) and #4 (V_4) due to electromagnetic coupling. Here, only the induced signals of the nearest-neighbor electrodes (#1 and #3) to the input channel (#2) are taken into account. The strength of electromagnetic coupling can be obtained by measuring the intensity ratio of the induced signal to the input calibration signal. If this procedure are similarly carried out for other electrodes, whole the calibration procedure can be easily performed to the BPM.

For simplicity, taking into account two transmission lines as the stripline electrodes to analyze the electromagnetic coupling between the electrodes, an equivalent model may be conceivable as shown in Fig. 3.

Here, taking into account proper symmetry, two calibrators in both the first and second transmission lines, V_{G1} and V_{G2}, respectively, are shown in Fig. 3, and the corresponding output impedances of the calibrators are Z_{G1} and Z_{G2},
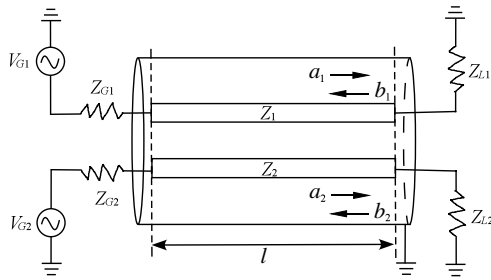
Figure 3: Equivalent model in the signal transmission lines of the BPM.

respectively. The characteristic impedances of the corresponding stripline electrodes are Z_1 and Z_2, respectively. The resistive terminated impedances of the corresponding transmission lines are Z_{L1} and Z_{L2}, respectively. The length of the transmission line is l. The normalized amplitudes of forward and backward waves transmitting along the stripline electrodes are indicated by a_i and b_i ($i = 1, 2$), respectively, and on these waves, detailed discussions are given in later section.

Equivalent Circuit

An equivalent circuit related to the equivalent model on the stripline-type BPM may be shown in Fig. 4. This equivalent-circuit model is based on a distributed-constant circuit model with distributed capacitances and inductances.
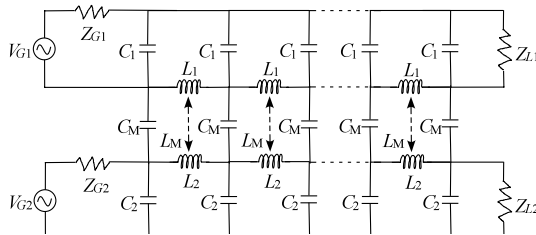

Figure 4: Equivalent circuit on two transmission lines with electromagnetic coupling.

Here, C_i and L_i ($i = 1, 2$) are a self-capacitance and a self-inductance per unit length in terms of the i-th stripline electrode without any electromagnetic coupling. C_M and L_M are a mutual-capacitance and a mutual-inductance per unit length between the two stripline electrodes. In such the equivalent circuit, quasi-TEM waves can propagate along the transmission lines with electromagnetic coupling [6]. In a case that resistive terminators matched to the characteristic impedance of the stripline electrode are applied at the downstream port of the electrodes, the forward waves are absorbed by the terminators, and however, the backward waves are generated at the downstream port due to electromagnetic coupling. On the other hand, in a case that the downstream port is short-terminated (or open) to the pipe ground, the forward waves are reflected and the backward waves propagate in the direction of the calibrator. Thus,

standing waves are excited along the stripline electrodes in spite of any type of the terminators at the downstream port.

THEORETICAL ANALYSIS

The quasi-TEM wave propagating along the stripline electrodes with electromagnetic coupling can be described with well-known telegraphic equations as follows [6]:

$$\frac{\partial V_1}{\partial z} = -L_1\frac{\partial I_1}{\partial t} - L_M\frac{\partial I_2}{\partial t}, \tag{1}$$

$$\frac{\partial I_1}{\partial z} = -C_1\frac{\partial V_1}{\partial t} + C_M\frac{\partial V_2}{\partial t}, \tag{2}$$

$$\frac{\partial V_2}{\partial z} = -L_2\frac{\partial I_2}{\partial t} - L_M\frac{\partial I_1}{\partial t}, \tag{3}$$

$$\frac{\partial I_2}{\partial z} = -C_2\frac{\partial V_2}{\partial t} + C_M\frac{\partial V_1}{\partial t}. \tag{4}$$

Here, V_i and I_i ($i = 1, 2$) are the voltage and current amplitudes in the i-th electrode at the position z and time t, respectively. When $C_M = 0$ and $L_M = 0$, the telegraphic equations are ascribed to simple equations related to the independent two stripline electrodes without any electromagnetic coupling. The theoretical analysis discussed here is briefly summarized, since a detailed analysis is available elsewhere [7].

The voltage and current amplitudes of the standing wave, $V_i(z)$ and $I_i(z)$($i = 1, 2$), are represented by using the relations, $V_i = V_i(z)e^{j\omega t}$ and $I_i = I_i(z)e^{j\omega t}$, respectively. Using the corresponding characteristic impedance Z_i for the i-th stripline electrode, the normalized amplitudes $a_i(z)$ and $b_i(z)$ of the forward and backward waves are given by

$$a_i(z) = \frac{V_i(z) + Z_iI_i(z)}{2\sqrt{2Z_i}}, \tag{5}$$

$$b_i(z) = \frac{V_i(z) - Z_iI_i(z)}{2\sqrt{2Z_i}}. \tag{6}$$

Solving Eqs. (5) and (6) inversely, the voltage and current amplitudes of the standing wave are represented by

$$V_i(z) = \sqrt{2Z_i}(a_i(z) + b_i(z)), \tag{7}$$

$$I_i(z) = \sqrt{\frac{2}{Z_i}}(a_i(z) - b_i(z)). \tag{8}$$

Here, taking into account only one calibrator, that is, $V_{G1} \neq 0$ and $V_{G2} = 0$, the boundary conditions at the end ports, $z = 0$ and $z = l$, are given by

$$V_1(0) + Z_{G1}I_1(0) = V_{G1}, \tag{9}$$

$$V_1(l) = Z_{L1}I_1(l), \tag{10}$$

$$V_2(0) + Z_{G2}I_2(0) = 0, \tag{11}$$

$$V_2(l) = Z_{L2}I_2(l). \tag{12}$$

Thus, taking into accout these boundary conditions, the telegraphic equations with electromagnetic coupling, Eqs. (1)−(4), can be directly solved. The results for the

first transmission line are given by

$$V_1(0) = \frac{1 + \Gamma_{L1}\zeta_1^{-2}}{1 - \Gamma_{G1}\Gamma_{L1}\zeta_1^{-2}}V, \qquad (13)$$

$$V_1(l) = \frac{\zeta_1^{-1}(1 + \Gamma_{L1})}{1 - \Gamma_{G1}\Gamma_{L1}\zeta_1^{-2}}V, \qquad (14)$$

and the results for the second transmission line are given by

$$V_2(0) = \left[\frac{\overline{\kappa}(\zeta_1^{-1} - \zeta_2^{-1})(\Gamma_{L1}\zeta_1^{-1} + \Gamma_{L2}\zeta_2^{-1})}{(1 - \Gamma_{G1}\Gamma_{L1}\zeta_1^{-2})(1 - \Gamma_{G2}\Gamma_{L2}\zeta_2^{-2})} \right. \\ \left. + \frac{\overline{\chi}(1 - \zeta_1^{-1}\zeta_2^{-1})(1 + \Gamma_{L1}\Gamma_{L2}\zeta_1^{-1}\zeta_2^{-1})}{(1 - \Gamma_{G1}\Gamma_{L1}\zeta_1^{-2})(1 - \Gamma_{G2}\Gamma_{L2}\zeta_2^{-2})}\right]V_{20}, \qquad (15)$$

$$V_2(l) = \left[\frac{\overline{\kappa}(\zeta_1^{-1} - \zeta_2^{-1})(1 + \Gamma_{L1}\Gamma_{G2}\zeta_1^{-1}\zeta_2^{-1})}{(1 - \Gamma_{G1}\Gamma_{L1}\zeta_1^{-2})(1 - \Gamma_{G2}\Gamma_{L2}\zeta_2^{-2})} \right. \\ \left. + \frac{\overline{\chi}(1 - \zeta_1^{-1}\zeta_2^{-1})(\Gamma_{L1}\zeta_1^{-1} + \Gamma_{G2}\zeta_2^{-1})}{(1 - \Gamma_{G1}\Gamma_{L1}\zeta_1^{-2})(1 - \Gamma_{G2}\Gamma_{L2}\zeta_2^{-2})}\right]V_{2l}. \qquad (16)$$

Here, the parameters ($i = 1, 2$) are defined by

$$\Gamma_{Li} \equiv \frac{Z_{Li} - Z_i}{Z_{Li} + Z_i}, \;\; \Gamma_{Gi} \equiv \frac{Z_{Gi} - Z_i}{Z_{Gi} + Z_i},$$

$$V \equiv \frac{(1 - \Gamma_{G1})}{2}V_{G1}, \;\; \zeta_i \equiv e^{j\beta_i l},$$

$$V_{20} \equiv (1 + \Gamma_{G2})V, \;\; V_{2l} \equiv (1 + \Gamma_{L2})V,$$

$$\overline{\kappa} \equiv \sqrt{\frac{Z_2}{Z_1}}\frac{\kappa}{\beta_1 - \beta_2}, \;\; \kappa \equiv \frac{1}{2}\sqrt{\beta_1\beta_2}\,(k_L - k_C),$$

$$k_L \equiv \frac{L_M}{\sqrt{L_1 L_2}}, \;\; k_C \equiv \frac{C_M}{\sqrt{C_1 C_2}},$$

where β_i is the uncoupled wave number in the i-th stripline electrode. It should be noted that k_L and k_C are the important parameters which represent the magnetic- and electric-coupling parameters between the stripline electrodes, respectively. Thus, Eqs. (13)−(16) give the analytical formula in the voltage amplitudes at the end ports of the stripline electrodes with any output impedances of the calibrators (Z_{G1}, Z_{G2}), any characteristics impedances of the transmission lines (Z_1, Z_2), and any resistive terminated impedances (Z_{L1}, Z_{L2}).

Here, taking into account symmetrical structure for the stripline electrodes short-terminated to the pipe ground, let's impose following restrictive conditions for the parameters, (i) $Z_{G1} = Z_{G2} = 50$ Ω, (ii) $Z_{L1} = Z_{L2} = 0$ Ω, (iii) $Z_1 = Z_2 = Z_0$, and $\beta_1 = \beta_2 = \beta \equiv \omega/v_0$ where ω and v_0 are the angular frequency and velocity of the propagating wave. Under these restrictive conditions, the voltage amplitudes at the downstream ports are modified according to

$$V_2(0) = \left[\frac{j\omega K_f(\Gamma_{L1} + \Gamma_{L2})\zeta^{-2}}{(1 - \Gamma_{G1}\Gamma_{L1}\zeta^{-2})(1 - \Gamma_{G2}\Gamma_{L2}\zeta^{-2})} \right. \\ \left. + \frac{K_b(1 - \zeta^{-2})(1 + \Gamma_{L1}\Gamma_{L2}\zeta^{-2})}{(1 - \Gamma_{G1}\Gamma_{L1}\zeta^{-2})(1 - \Gamma_{G2}\Gamma_{L2}\zeta^{-2})}\right]V_{20}, \qquad (17)$$

$$V_2(l) = \left[\frac{j\omega K_f(1 + \Gamma_{L1}\Gamma_{L2}\zeta^{-2})\zeta^{-1}}{(1 - \Gamma_{G1}\Gamma_{L1}\zeta^{-2})(1 - \Gamma_{G2}\Gamma_{L2}\zeta^{-2})} \right. \\ \left. + \frac{K_b(1 - \zeta^{-2})(\Gamma_{L1} + \Gamma_{G2})\zeta^{-1}}{(1 - \Gamma_{G1}\Gamma_{L1}\zeta^{-2})(1 - \Gamma_{G2}\Gamma_{L2}\zeta^{-2})}\right]V_{2l}. \qquad (18)$$

Here, the parameters are defined by

$$K_f \equiv -\frac{\kappa l}{\omega}, \;\; K_b \equiv \frac{\chi}{2\beta}, \;\; \zeta_1 = \zeta_2 = \zeta \equiv e^{j\beta l},$$

$$\overline{\chi} \equiv \sqrt{\frac{Z_2}{Z_1}}\frac{\chi}{2\beta}, \;\; \chi \equiv \frac{1}{2}\beta\,(k_L + k_C).$$

Under these restrictive conditions, assuming that the velocity of the propagating wave is equal to the velocity of light ($v_0 = c$), the parameters k_L, k_C, l and Z_0 are the free ones to be experimentally determined. These free parameters can be quantitatively obtained on the base of a least-squares fitting procedure using the analytical formulae Eq. (17). The experimental tests can be systematically performed with an rf network analyzer which can measure S-parameters. The electromagnetic coupling strength C_s is directly related to the parameter S_{21} as follows:

$$C_s = \left|\frac{V_2(0)}{V_{G1}}\right|, \qquad (19)$$

$$S_{21} = 20\log_{10}C_s. \qquad (20)$$

EXPERIMENTAL TESTS

Characteristic Measurements

Using an rf network analyzer, the coupling strength between the stripline electrodes #2 (input port) and #1 (or #3) (output port) was obtained by measuring the parameter S_{21} in frequency domain (see Fig. 2) in which the frequency region is from 10 MHz to 1.2 GHz. The results are shown in Fig. 5. Figures 5(a) and 5(b) show the measurement results of the amplitude and the phase in the parameter S_{21} between the stripline electrodes #2 and #1, respectively, where the experimental data are indicated with cross points. The solid lines represent fittings of the experimental data using the analytical formulae (Eq. (17)) based on a least-squares fitting procedure, and the broken lines indicate calculations with the different parameters on k_L while the other fitted parameters are fixed. The similar results were obtained for those between the stripline electrodes #2 and #3.

In Fig. 5(a) we can see a well-known resonant structure in frequency domain in the amplitude of the parameter S_{21} measurement due to the excitation of a standing wave on the stripline electrodes. The dip frequency f_d at the central region is 538.2 MHz. The frequency f_m giving the maximal sensitivity (or the maximal coupling strength) and the amplitude of the parameter S_{21} are 315.8 (837.1) MHz and −39.7 (−36.4) dB in the first (second) lobe, respectively. The coupling strength is $C_s \sim 1\%$ while f_m in the first lobe is very close to the frequency ($f = 300$ MHz) of the on-board calibrator under development for the new detection electronics.
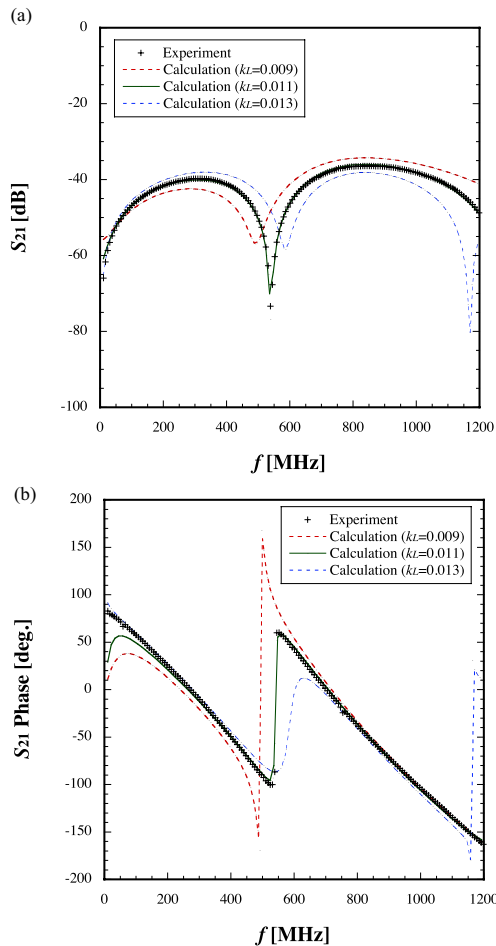
(a)

(b)

Figure 5: Measurement results of the parameter S_{21}, (a) the amplitude and (b) the phase. It should be noted that the phase is defined in the region within ± 180 º.

The coupling strength obtained for the new BPM is about one-eighth smaller than that for the present BPM [5]. The results may come from (i) the elongation of the length between the stripline electrodes due to the increase of the BPM aperture, (ii) the reduction of the angular width of the electrode, and (iii) the coupling strength is reduced due to the different mechanical structure of the stripline electrode compared with that of the present BPM. The third item is in detail discussed in later section.

Characteristic Analysis and Discussions

The characteristic analysis was performed for the free parameters based on a least-squares fitting procedure with the analytical formula. The results are obtained to be $k_L = 0.011$, $k_C = 0.013$, $Z_0 = 42.5$ Ω, and $l = 128.1$ mm. In Figs. 5(a) and 5(b), the calculated lines are obtained depending on the magnetic-coupling parameter k_L while the other fitted parameters are fixed. The experimental results are in good agreement with calculations. The characteristic impedances of the stripline electrodes were directly measured to be $Z_0 = 41 \pm 2$ Ω with a time-domain reflectometer (TDR). The measurement result is also in good agree-

ment with this characteristic analysis. It should be noted that the measurement results with a TDR give the characteristic impedance under a condition with electromagnetic coupling between the four stripline electrodes, while the characteristic analysis gives the characteristic impedance Z_0 as a free parameter under a condition without any electromagnetic coupling. However, the difference is quantitatively small within experimental errors. Thus, the characteristic analysis is satisfactory enough with the experimental results.

On the length of the stripline electrode, the mechanical length of the transmission line for the stripline electrode is $l = 132.5$ mm, is slightly different from the electric length of $l = 128.1$ mm obtained by the characteristic analysis. This may come from slight electromagnetic distortion of the propagating quasi-TEM wave at the end ports because the characteristic analysis is simply based on an analysis in one dimension, and thus, it should be carried out by taking into account more rigorous electromagnetic distortions at the end ports in three dimensions.

The results also show that the magnetic-coupling parameter k_L is smaller than the electric one k_C by $\sim 15\%$. It can be understood that because the inner radius of the stripline electrode is the same as the pipe radius without any mechanical steps away from the inner surface of the pipe, the magnetic-coupling strength may be reduced in comparison with the electric one.

Again, in Fig. 5(a) we can clearly see a slight asymmetry in the resonant structure in terms of the dip frequency, and also see an asymmetric structure even in each lobe. These results have not been observed at all in the present BPM for which $k_L \simeq k_C$. The results in the phase of the parameter S_{21} measurement are shown in Fig. 5(b). The experimental results are also in good agreement with calculations.

CONCLUSIONS

We have successfully tested a new stripline-type BPM with a large aperture for analyzing electromagnetic coupling between the stripline electrodes. The coupling strength was measured to be $\sim 1\%$. With the analytical model based on a coupled-mode theory in transmission lines with electromagnetic coupling, the experimental results are in good agreement with calculations.

REFERENCES

[1] M. Masuzawa, Procs. the First International Particle Accelerator Conference (*IPAC'10*), KICC, Kyoto, 2010, p. 4764.

[2] R.E. Shafer, AIP Conf. Proc. 212, 26 (1990).

[3] S.R. Smith, AIP Conf. Proc. 390, 50 (1997).

[4] E. Medvedko *et al.*, Procs. the 2008 Beam Instrumentation Workshop (*BIW08*), Lake Tahoe, California, 2008, p. 190.

[5] T. Suwada *et al.*, Nucl. Instr. and Meth. A 440 (2000) 307.

[6] B.M. Oliver, Procs. the I.R.E., Vol. 42, Nov. (1954) 1686.

[7] S.J. Orfanidis, *Electromagnetic Waves and Antennas*, p. 456 (2010) (see http://www.ece.rutgers.edu/~orfanidis/ewa).